Semi-Circular Array Antennas for DOA-Estimation and Beamforming

J. Freese*, Ch. Müller, M. Schüßler, and R. Jakoby
Technische Universität Darmstadt, Inst.f.Hochfrequenztechnik,
Merckstraße 25, 64283 Darmstadt, Germany. freese@hf.tu-darmstadt.de

Abstract

In this contribution, the application of two semi-circular array antennas, consisting of monopoles and microstrip patches backed by a metallic reflector are investigated for smart antenna systems with a wide angular-operating range. The pattern of the monopoles or patches depends upon the respective position in the array. Therefore, and due to the nonlinear arrangement of the elements, a transformation to an alternative manifold is needed prior to the usual signal processing techniques. The investigated transformations are based on the least-mean squares solution of an over-determined set of equations and they already include the calibration in case of measured data. The transformation is successfully applied to theoretical and measured array steering vectors within a predefined angular-operation range of ±78°.

Introduction

In smart antenna systems, typical array configurations are linear, rectangular or circular, having array elements with identical radiation pattern. Then, the overall radiation pattern of the array is the product of the element factor and the array factor, where the element pattern basically limits the angular-operating range of the array. To overcome this limitation, arrays with different elements may be used. The transformation schemes, which are discussed in this paper, are needed because the usual signal processing techniques can not directly be applied to such arrays. The investigated array configurations are a Semi-Circular Monopole Array (SCMA) and a Semi-Circular Microstrip Patch Array (SCPA), both backed by a metallic reflector. The realized SCMA in Fig. 1 and the SCPA in Fig. 2 consist of eight monopoles and eight series-fed microstrip patch rows, respectively. Both are designed to operate at 10 GHz.

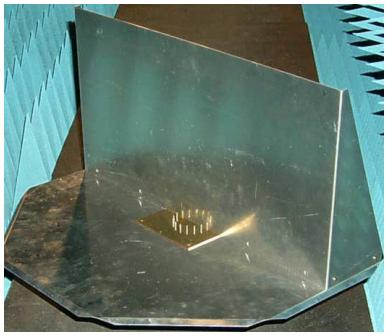

Fig. 1: Semi-circular array of eight monopoles (SCMA).

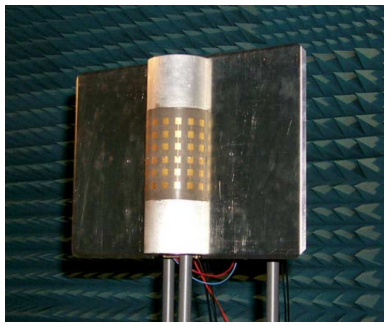

Fig. 2: Semi-circular array of eight series-fed patch rows (SCPA).

Individual Element Pattern

To compare the two different arrays, all pattern functions are assumed to be independent of the elevation angle Θ and investigated only in azimuth. The azimuth plane is the *xy*-plane, the *z*-axis is parallel to the cylinder axis, and the *x*-axis, i.e. $\Theta=\pi/2$ and $\Phi=0$, is perpendicular to the reflector.

The omnidirectional monopole and the image source caused by the reflector results in an element pattern $g_n(\Phi)$ of the monopoles in the SCMA that is simply a sine function, depending upon the radius ρ and the angular position Φ_n of the monopoles within the circular array. The radius is chosen to be λ_0 to achieve a spacing below $\lambda_0/2$ along the

circumference. For the pattern of the elements in the SCPA, use is made of the approximation according to [1]. The radius of the SCPA is $1.67\lambda_0$, yielding an element spacing of about $0.7\lambda_0$. The theoretical element pattern are depicted in Fig. 3 for the four elements on the upper quadrant of the realized arrays. Because of symmetry, the elements on the lower quadrant show the same, but mirrored characteristics.

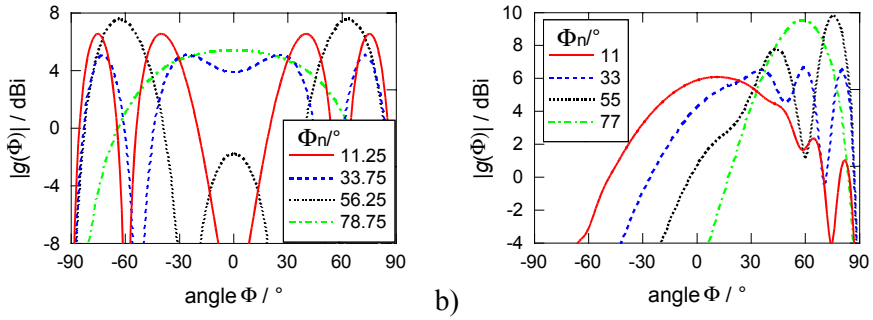

Fig. 3: Magnitude of the theoretical element pattern $g(\Phi)$ for four of the eight elements of the a) SCMA and b) SCPA. Φ_n describes the element´s angular position.

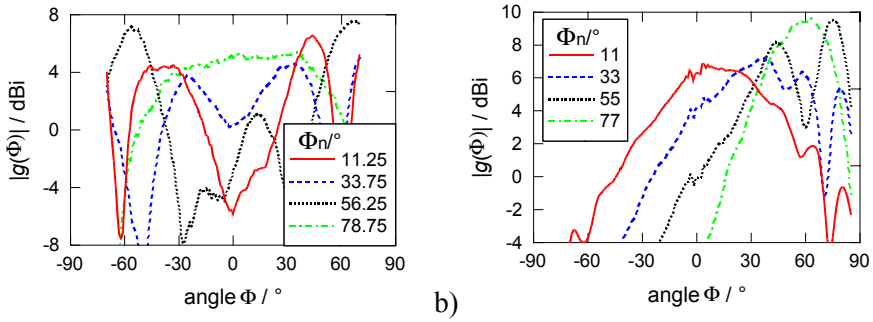

Fig. 4: Magnitude of the measured element pattern $g(\Phi)$ for four of the eight elements of the a) SCMA and b) SCPA. Φ_n describes the element´s angular position.

Fig. 4 exhibits the measured element pattern of the realized arrays, which are characterized by a X-Band multi-channel measurement receiver. The comparison with the theoretical pattern indicates a good agreement, where the small differences between the plots are mainly due to the finite size of the reflector and mutual coupling, that shows a stronger influence in the SCMA than in the SCPA.

Angular-Operation Range

Prior to the transformation an Angular-Operation Range (AOR) is defined in which the transformation should work. For this purpose an optimum weight vector $\boldsymbol{w}$ and the corresponding far-field pattern is determined for scanning directions $-\pi/2 \le \Phi_0 \le \pi/2$:

$$F(\Phi_0) = \boldsymbol{w}^H \cdot \boldsymbol{a}(\Phi_0)\,. \qquad (1)$$

The steering vector $\boldsymbol{a}$ of the semi-circular array with the element pattern $g_n(\Phi)$ is:

$$\boldsymbol{a}(\Phi) = \left[a_1(\Phi) \cdots a_N(\Phi)\right]^T \qquad a_n(\Phi) = g_n(\Phi) \cdot e^{j2\pi\rho/\lambda_0 \cdot \cos(\Phi - \Phi_n)}. \qquad (2)$$

According to the beamforming method proposed in [2], the optimum weight vector is:

$$\boldsymbol{w} = \boldsymbol{R}^{-1}\boldsymbol{a}(\Phi_0) = \boldsymbol{R}^{-1}\boldsymbol{a}_0\,. \qquad (3)$$

In contrast to [2], a continuous noise environment with a uniform noise distribution $\sigma^2 = N_0/(4\pi)$ is assumed here. If the steering vector is independent of Θ and the azimuthal angular range is $-\pi/2 \le \Phi \le \pi/2$, the elements r_{uv} of $\boldsymbol{R}$ are determined by:

$$r_{uv} = \frac{N_0}{2\pi} \int_{-\pi/2}^{\pi/2} a_u a_v^* d\Phi \,, \tag{4}$$

where a_n are the elements of the steering vector. For some ideal array configurations this integral may be solved analytically. It is interesting to note, that for a simple linear array of isotropic radiators, spaced in $\lambda_0/2$ distances, $\boldsymbol{R}$ is a multiple of the unity matrix and the optimal antenna weight vector $\boldsymbol{w}$ is proportional to the steering vector $\boldsymbol{a}(\Phi_0)$ of the desired scan direction. This corresponds to the matched filter solution, assuming uncorrelated noise in the receiver branches. However, especially in the case of measured steering vectors, Eq. (4) has to be solved numerically.
To assess the AOR of the investigated arrays, the achievable directivity D_0 is determined from Eq. (1) for each scanning angle Φ_0. The achieved mean value of the directivity is about 12.3 dBi ± 0.7 dBi within a sector of ±78° for both arrays. This sector defines the AOR of the SCMA and the SCPA for the following transformation.

Transformation
The transformation method proposed in [3] is based on the principle of phase-mode excitation and determines a transformation matrix $\boldsymbol{T}$ analytically to map the steering vector $\boldsymbol{a}$ of a circular array to the manifold

$$\boldsymbol{a_{BSM}}(\Phi) = \boldsymbol{T} \cdot \boldsymbol{a} = \left[e^{-jM\Phi} \cdots \; e^{-j\Phi} \; 1 \; e^{j\Phi} \cdots \; e^{jM\Phi} \right]^T . \tag{5}$$

The vector $\boldsymbol{a}_{BSM}(\Phi)$ is the steering vector of a so called beam-space manifold (BSM). The number of phase modes M that are considered depends upon the array radius and is chosen to be M=5 for the SCMA and M=6 for the SCPA. DOA-estimation algorithms, e.g. MUSIC, can be applied to this manifold in the same way as for linear arrays, because the steering vector $\boldsymbol{a}_{BSM}$ shows the same structure [3]. For beamforming purposes, the optimum weights for this manifold are determined with Eq. (4) and the elements of the matrix $\boldsymbol{R}$ are given by

$$r_{uv} = N_0/2 \cdot \mathrm{si}\left(\pi(u-v)/2\right) \qquad u,v = 1 \ldots M \,. \tag{6}$$

For the investigated semi-circular arrays there is no analytical solution for the transformation matrix $\boldsymbol{T}$ and a best-fit approximation shall be found. Therefore, the steering matrices

$$\boldsymbol{A} = \left[\boldsymbol{a}(\Phi_1) \quad \cdots \quad \boldsymbol{a}(\Phi_L) \right], \qquad \boldsymbol{A_{BSM}} = \left[\boldsymbol{a_{BSM}}(\Phi_1) \quad \cdots \quad \boldsymbol{a_{BSM}}(\Phi_L) \right] \tag{7}$$

are composed from steering vectors at L reference angles and the equation

$$\boldsymbol{A_{BSM}} = \boldsymbol{T} \cdot \boldsymbol{A} \tag{8}$$

is solved in a least-mean squares sense by the pseudo inverse of $\boldsymbol{A}$:

$$\boldsymbol{T_A} = \boldsymbol{A_{BSM}} \cdot \boldsymbol{A^H} \cdot \left(\boldsymbol{A A^H} \right)^{-1} . \tag{9}$$

To evaluate the performance of the transformation, the error function $err(\Phi)$ is used:

$$err(\Phi) = \frac{1}{M} \sum_{m=1}^{M} \left| \Delta_m(\Phi) \right|, \quad \boldsymbol{\Delta}(\Phi) = \boldsymbol{a}_{BSM}(\Phi) - \boldsymbol{T}\boldsymbol{a}(\Phi) = \left[\Delta_1(\Phi) \ldots \Delta_M(\Phi) \right]^T \tag{10}$$

As shown in Fig. 5, the transformation works for the SCMA, indicating a mean error of only 5%, whereas the resulting mean error of about 22% for the SCPA is too large. Therefore, a second scheme is proposed here, aiming to reduce this error. A new matrix $\boldsymbol{B}$ is composed from the real and the imaginary part of the steering matrix $\boldsymbol{A}$:

$$\boldsymbol{B} = \begin{bmatrix} \Re\{\boldsymbol{A}\} \\ \Im\{\boldsymbol{A}\} \end{bmatrix} \tag{11}$$

In Eq. (9), $\boldsymbol{A}$ is then replaced by $\boldsymbol{B}$ to determine $\boldsymbol{T_B}$ instead of $\boldsymbol{T_A}$. This transformation scheme yields much better results, reducing the mean error down to 1% for the SCPA.

Because the inversion of $\boldsymbol{BB}^H$ is not possible, this scheme can not be applied to the theoretical steering vector of the SCMA.

To compensate mutual coupling and other electromagnetic effects, that are included in real antenna systems, different calibration algorithms have been proposed, e.g. the method in [4] which is based on a least-mean squares solution, too. The presented transformation includes the calibration, because it maps a measured steering vector to an error-free BSM steering vector.

The resulting error after the transformation of the measured values with both proposed schemes is shown in Fig. 6. When the measured values for the SCMA are used, the inversion of $\boldsymbol{BB}^H$ is possible. The second transformation scheme that uses the separate real and imaginary part of the measured steering vectors reaches a mean error of 3% and 10% for the SCMA and the SCPA, respectively, which is significantly lower for both arrays compared to the first scheme.

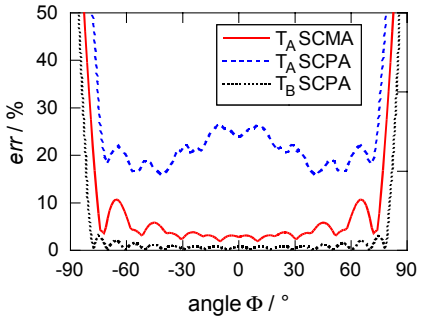

Fig. 5: Transformation error for the theoretical steering vectors.

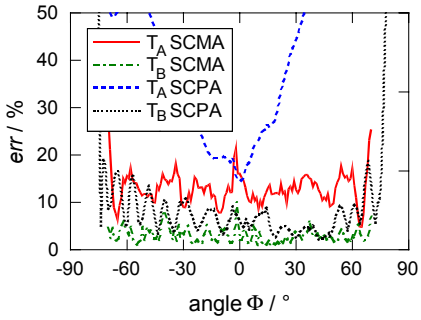

Fig. 6: Transformation error for the measured steering vectors.

Conclusions

Two transformation schemes have been discussed for the application of semi-circular array configurations with different elements in smart antenna systems. The investigated arrays, the SCMA and SCPA consist of monopoles or microstrip patches, respectively, both backed by a metallic reflector. The theoretical and measured element pattern, that depend upon the element´s angular position in the array, are in good agreement. A a wide angular-operating range of ±78° is defined in which a directivity of 12.3 dBi ± 0.7 dBi is achieved. The first transformation scheme works well for the theoretical steering vectors of the SCMA but it fails for the SCPA. The second transformation scheme works with separated real and imaginary parts of the steering vectors. It is successful for the theoretical values of the SCPA but it can not be applied to the SCMA. However, the transformation of the measured steering vectors, that includes the calibration, with the second scheme yields by far the best results for both arrays. Hence, it is assumed that this scheme may significantly improve the transformation and calibration results for other array configurations, too.

References

[1] Freese, J.; Tudosie, G.; Schüßler, M.; Jakoby, R.: Semi-Circular Microstrip Array on a Planar Reflector with Extended Beam-Scanning Range. Proceedings of the IEEE APS/URSI Symposium, June 22-27, 2003, Columbus, Ohio, USA.

[2] Sureau, J.; Keeping, K. J.: Sidelobe control in cylindrical arrays. IEEE Trans. on Antennas Propagation, Vol. 30, September 1982, pp. 1027 – 1031.

[3] Mathews, C. P.; Zoltowski, M. D.: Eigenstructure Techniques for 2-D Angle Estimation with Uniform Circular Arrays. IEEE Trans. on Signal Processing, Vol. 42, September 1994, pp. 2395 –2407.

[4] Pierre, J., Kaveh, M.: Experimental Performance of Calibration and Direction-Finding Algorithms. Proc. IEEE ICCASP, Toronto, Canada (1991), S. 1365-1368.